Reliable Measurement of Cortical Flow Patterns using Complex Independent Component Analysis of Electroencephalographic Signals

Jörn Anemüller, Terrence J. Sejnowski, and Scott Makeig

Swartz Center for Computational Neuroscience, Institute for Neural Computation,
University of California San Diego, La Jolla, California, and
Computational Neurobiology Laboratory,
The Salk Institute for Biological Studies, La Jolla, California

Abstract. Complex independent component analysis (ICA) of frequency-domain electroencephalographic (EEG) data [1] is a generalization of real time-domain ICA to the frequency-domain. Complex ICA aims to model functionally independent sources as representing patterns of spatio-temporal dynamics. Applied to EEG data, it may allow non-invasive measurement of flow trajectories of cortical potentials. As complex ICA has a higher complexity and number of parameters than time-domain ICA, it is important to determine the extent to which complex ICA applied to brain signals is stable across decompositions. This question is investigated for the complex ICA method applied to the 5-Hz frequency band of data from a selective attention EEG experiment. [1]

1 Complex ICA of frequency-domain EEG signals

The goal of complex ICA for frequency-domain EEG signals [1] is to replace the standard static source model with a more dynamic one that allows modeling each source as having a spatio-temporally varying activation pattern. The spatio-temporal dynamics of each source may be the result of, e.g., the spatial propagation of neural activity across the cortex, as observed in invasive animal recordings [2]. In contrast, instantaneous time-domain ICA would at best be able to approximate spatio-temporal source dynamics by one or more static ICA sources.

Taking into account spatio-temporal dynamics of sources leads to a convolutive model of source signal superposition, expressed in the frequency-domain as instantaneous mixing with complex-valued superposition coefficients that vary across frequencies. The frequency-domain approach to EEG signal analysis allows different dominant functional sources in different frequency bands—an observation supported by the functionally distinct frequency bands observed in human EEG [3].

Here, we give a brief overview of the processing stages of the complex ICA algorithm for EEG signals, cf. Fig. 1. For a detailed description, the reader is referred to [1]. The measured EEG data $\mathbf{x}(t) = [x_1(t), \ldots, x_M(t)]^T$ are first transformed into the frequency-domain using the standard techniques of short-time Fourier or wavelet decomposition. This yields the spectral data $\mathbf{x}(T, f) = [x_1(T, f), \ldots, x_M(T, f)]^T$, where

[1] Supported by the German Research Council DFG (J. A.), and by the Swartz Foundation.

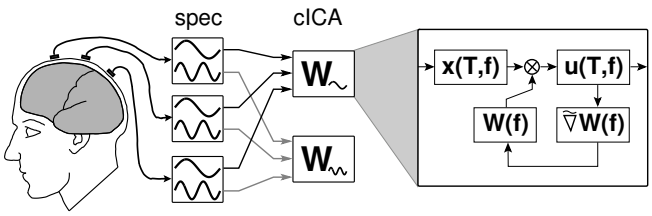

Fig. 1. Schematic representation of the processing stages of the complex frequency-domain ICA algorithm. Left ('spec'): the recorded electrode signals are decomposed into different spectral bands. Center ('cICA'): Complex ICA decomposition is performed within each spectral band. Right: Iteration steps performed by complex ICA for estimation of each separating matrix $\mathbf{W}(f)$.

f denotes frequency, and T denotes temporal position of the analysis window center. The goal of the complex ICA decomposition is to find for each frequency f a complex matrix $\mathbf{W}(f)$ that decomposes the measured signals $\mathbf{x}(T,f)$ into signals

$$\mathbf{u}(T,f) = \mathbf{W}(T)\,\mathbf{x}(T,f) \tag{1}$$

so that the components of $\mathbf{u}(T,f) = [u_1(T,f),\ldots,u_M(T,f)]^T$ are statistically independent. In practice, full independence usually cannot be achieved under the linear separation model (1). Rather, the decomposition makes the signals $\mathbf{u}(T,f)$ as independent as possible. The matrix $\mathbf{W}(f)$ may be estimated using a complex generalization of the infomax ICA algorithm. For details, see [1]. We have found that, applied to data from a visual selective attention experiment, complex ICA separates physiologically plausible components while achieving a higher degree of independence between signal components in each frequency band.

The improved quality of signal separation is largely due to the higher number of degrees of freedom in the complex algorithm, allowing one complex matrix per frequency band, as opposed to standard time-domain ICA which estimates a single real-valued matrix for the entire data. The question of reliability may be particularly important for the complex ICA algorithm since the increased number of parameters to be estimated might lead to instability of the obtained solutions under perturbations of the data or internal algorithm parameters.

In the remainder of the paper, we drop the frequency index f (i.e., $\mathbf{u}(T) \equiv \mathbf{u}(T,f)$ etc.), since reliability is evaluated separately for each frequency band.

2 Reliability analysis of complex independent components

Before introducing the approach for the reliability analysis of complex ICA, we briefly review previous work on the reliability analysis of real-valued ICA decompositions. Meinecke et al. [4] used resampling methods to study the stability of blind source separation (BSS) algorithms. This approach may be characterized as a 'local' approach: The original data were first decomposed into separated component signals. Then, bootstrap data sets were generated from the *separated* signals and again decomposed. The obtained separating matrices were characterized by 'small deviations from the identity

matrix in every Bootstrap sample' [4]. Meinecke et al. analyzed 8-channel electrocardiographic (ECG) data and 49-channel magnetoencephalographic (MEG) data that were projected to the first 23 and 25 principal component subspaces, respectively, during preprocessing. Only a few reliable one-dimensional components were obtained (2 and 3, respectively, as mentioned in [4]). Signal subspaces with multidimensional components were also found, a case not investigated in the present paper.

Recently, Duann et al. [5] studied the reliability of real infomax ICA [6] using functional magnetic resonance imaging (fMRI) data. Variability was induced by different random shuffling of the training data order in ten repeated decompositions, so that the algorithm's gradient update steps were applied to the data in different orders in different decompositions. This approach may be characterized as testing 'global' reliability: The ICA algorithm was applied to the mixed data, resulting in convergence to solutions in which the same ICA components could occur in different orders in different decompositions. Matching components between pairs of ICA decompositions, Duann et al. obtained most consistent results using a correlation criterion. The 600 dimensional recorded data were projected onto their first 100 principal components during preprocessing. All 100 separated components were reliably reproduced in each run of the algorithm.

To analyze the reliability of complex ICA [1], we generalize the 'global' approach of [5] to complex data, repeating decompositions on mixed data and finding best-matching components in different decompositions after training.

We investigate three sources of variability as test conditions:

Bootstrap data selection. We generate R bootstrap data sets $\mathbf{x}^{(r)}(T)$, $r = 1, \ldots, R$, from the original data set $\mathbf{x}^{(o)}(T)$ by drawing (with replacement) each sample of $\mathbf{x}^{(r)}(T)$ at random from the original data set. The bootstrap sets have same size as the original set. Complex ICA is performed on the original and on each of the bootstrap data sets, yielding independent components $\mathbf{u}^{(o)}(T), \mathbf{u}^{(1)}(T), \ldots, \mathbf{u}^{(R)}(T)$. The initial estimate of the separating matrix is the identity matrix for each decomposition. This condition tests the stability of the algorithm with respect to small variations in the data, i.e., it allows us to assess how stable the algorithm is with respect to data generated from the same (empirical) distribution.

Training data order selection. Our implementation of the complex ICA algorithm performs optimization in a semi-online fashion on small blocks of data points, in the same way as the standard implementation of the infomax ICA algorithm [5,7]. The order in which data points are used for gradient evaluation is chosen at random prior to each sweep through the whole data, and could affect optimization and convergence. To test variability with respect to this training data shuffling, we perform complex ICA decompositions of the original data set $\mathbf{x}^{(o)}(T)$ for R different seed settings of the random number generator that generates the shuffling. Hence, the training data order is different for each of the R decompositions, resulting in independent components $\mathbf{u}^{(1)}(T), \ldots, \mathbf{u}^{(R)}(T)$. Again, the initial estimate of the separating matrix is chosen as the identity matrix for each decomposition. The training data order condition tests the stability of the implementation's gradient optimization procedure.

Weight initialization selection. The complex ICA algorithm uses by default the identity matrix as the initial estimate of the separating matrix. To test variability with respect

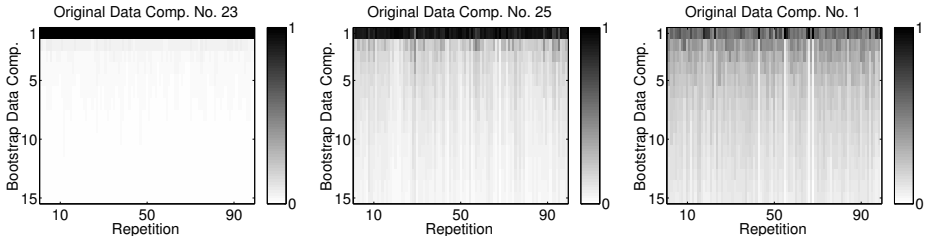

Fig. 2. Effectiveness of the method employed for matching components in different repetitions of the ICA decomposition. For three components obtained from the original data set (from left to right: 23, 25, 1), and for each of the 99 bootstrap data sets (abscissa), the graphs display the correlation coefficients for the 15 (out of 31) bootstrap data set components (ordinate) that had highest correlations with the original data set component. Each column was sorted from highest (top) to lowest (bottom). In each repetition, the bootstrap component with the highest correlation (row 1), was defined as best-matching the original component. Original components 23 (left) and 25 (center) had median correlation coefficients of 0.9996 and 0.9112, respectively, with their best-matching bootstrap components. These values correspond to the highest and lowest correlation values among components found as reliable (i.e., having a median correlation coefficient of 0.9 or higher). Original component 1 (right) had median correlation coefficient of 0.5761 with its best-matching bootstrap components, corresponding to the smallest correlation value of all (unreliable) components. Since except for outliers the best-matching bootstrap components (top row) for the reliable components (left and center panels) show significantly higher correlation than their next-best matching bootstrap components (rows 2 to 15), the employed scheme for matching components is appropriate.

to this initial condition, we generate R initialization matrices $\mathbf{W}_{\text{init}}^{(r)}$, $r = 1,\ldots,R$, with coefficients drawn randomly from a Gaussian distribution with zero mean and unit variance, resulting after decompositions in independent components $\mathbf{u}^{(1)}(T),\ldots,\mathbf{u}^{(R)}(T)$. The original data set $\mathbf{x}^{(o)}(T)$ is used as input, and the same training data order is used for all R decompositions. The initialization condition tests the ability of the gradient-based optimization to escape local minima and find global minima.

Complex independent components obtained, in any of the three conditions, with repeated decompositions may occur in different orders in different decompositions due to the permutation invariance of the ICA solution. Therefore, pairs of best-matching components in the original decomposition $\mathbf{u}^{(o)}(T)$ and each repeated decomposition $\mathbf{u}^{(r)}(T)$ must be found. Because of the scaling invariance of the ICA problem, corresponding components may differ by an unknown scaling factor, which in the complex case includes an arbitrary phase shift (i.e., multiplication by a unit-norm complex number). To find best-matching components, we employ the complex correlation coefficient of their activity time courses, similar to the procedure that has been determined in [5] as optimal for real-valued components. Define as $\mathbf{u}^{(o)}(T)$ the components obtained from the original data $\mathbf{x}^{(o)}(T)$ with original training data order and identity matrix initialization $\mathbf{W}_{\text{init}}^{(o)} = \mathbf{I}$. Denote by $\mathbf{u}^{(r)}$ the components obtained from the r-th repetition in one of the three investigated conditions. We compute for all repetitions r the correlation matrix $\mathbf{C}^{(r)}$ with (i,j)–entry

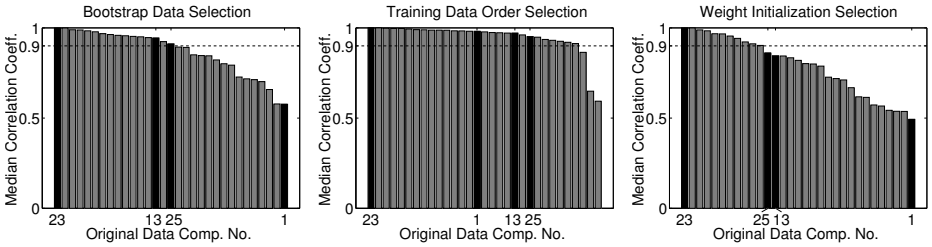

Fig. 3. Reliability of the obtained components. The median correlation coefficient (ordinate) of each original data set component's (abscissa) time course with its best-matching bootstrap data set components is shown for bootstrap data (left), training data order (center), and weight initialization selection (right), respectively. Components were sorted from highest correlation (left) to lowest (right). Components used as examples in this manuscript are marked by black bars, with their component number in the original data set decomposition indicated on the abscissa. Using a threshold of a minimum 0.90 median correlation coefficient (dashed line) for reliability, the training data order condition (center) yielded the highest number of reliable components (28 out of 31), bootstrap data (left) produced 16 reliable components, and weight initialization 11 (right).

$$\left[\mathbf{C}^{(r)}\right]_{ij} = \rho_{ij}^{(r)} = \left| \left\langle u_i^{(o)}(T) \left(u_j^{(r)}(T)\right)^* \right\rangle_T - \mu_i^{(o)} \left(\mu_j^{(r)}\right)^* \right| / \left[\sigma_i^{(o)} \sigma_j^{(r)}\right] \tag{2}$$

corresponding to the magnitude correlation coefficient of component i in the original decomposition and component j in the r-th repeated decomposition. Here, $\langle\cdot\rangle_T$ denotes expectation computed as time average; $*$ complex conjugation; $|\cdot|$ magnitude; and $\mu_i^{(o)}$, $\sigma_i^{(o)}$ and $\mu_j^{(r)}$, $\sigma_j^{(r)}$ denote mean and standard deviation of the i-th original component and of the j-th component of the r-th repetition, respectively. For each repetition r and each original data component i, we assign component $\tilde{j}$,

$$\tilde{j}(i,r) = \underset{j}{\operatorname{argmax}} \left(\rho_{ij}^{(r)}\right), \tag{3}$$

that has maximum correlation coefficient as the best-matching component for original component i. Component $u_i^{(o)}(T)$ is considered 'reliable' if the median (across repetitions) correlation coefficient with its matching components,

$$\tilde{\rho}_i = \underset{r}{\operatorname{median}} \left(\rho_{i,\tilde{j}(i,r)}^{(r)}\right) \tag{4}$$

reaches or exceeds a chosen threshold value $\tilde{\rho}_{\text{thresh}}$.

3 Experiment paradigm

We employed complex ICA [1] to analyze data from a visual spatial selective attention experiment in which the subject was asked to respond by a button press as quickly as possible each time a target stimulus appeared in an attended location [7]. Analysis included 582 trials, each 1 s long, time locked to target stimulus presentations to

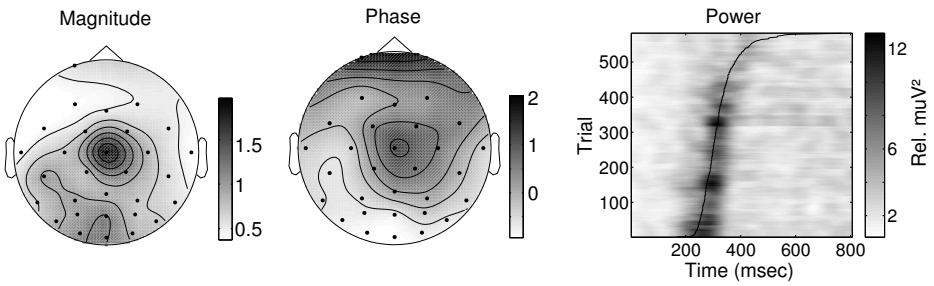

Fig. 4. Component 13 of the 5-Hz band represents a component whose activity was tightly linked to subject behavior (button press). It proved reliable in the bootstrap data and training data order conditions, and was just below the reliability threshold in the weight initialization condition. The graphs show (from left to right) the magnitude of the associated complex scalp map, the scalp map's phase, and the ERP-image plot of 5-Hz component signal power in different experimental trials (ordinate) and times after stimulus onset (abscissa). Subject response time in each trial is overlaid on the ERP image (black trace). For better visualization, the ERP image has been smoothed across trials with a 30-trials wide rectangular window. The impression of temporal smearing is induced by the length (200 ms) of the spectral decomposition window. The ERP image shows that component energy is maximum at the subject response time. The best-matching component obtained by real time-domain ICA did not show such a tight relationship to behavior (data not shown here). The component map exhibits a phase gradient around the central focus of activation, that reflects spatio-temporal dynamics of the underlying cortical activation.

one subject. The data were recorded from 31 EEG electrodes at a sampling rate of 256 Hz. Spectral decomposition was performed with a hanning-windowed Fourier basis of length 50 samples, with a window shift of 1 sample between successive analysis windows. Reliability analysis was confined to data in the 5-Hz band, due to processing limitations. For each of the three conditions (bootstrap data, training data order, and weight initialization selection), $R = 99$ decompositions were performed, each resulting in 31 complex independent components. In the bootstrap data condition, $R = 99$ bootstrap data sets were generated from the original 5-Hz band data after spectral decomposition. The 5-Hz original and bootstrap data, respectively, were sphered during preprocessing. The adaptation rate of the complex ICA algorithm was lowered successively, and optimization was halted when the total weight-change induced by one sweep through the data was smaller than 10^{-6} relative to the Frobenius norm of the weight-matrix. Convergence was attained in each decomposition within 222 iterations or less. To define component reliability, a minimum median correlation coefficient $\tilde{\rho}_{\text{thresh}} = 0.90$ was chosen, as suggested by the results presented in Figs. 2 and 3.

4 Results

The main results are presented in Figs. 2 to 5. Assigning best-matching complex components in different decompositions by means of the correlation coefficient between component activities is an appropriate method of identifying reliable components. The correlation of a reliable component with its best-matching component in different de-

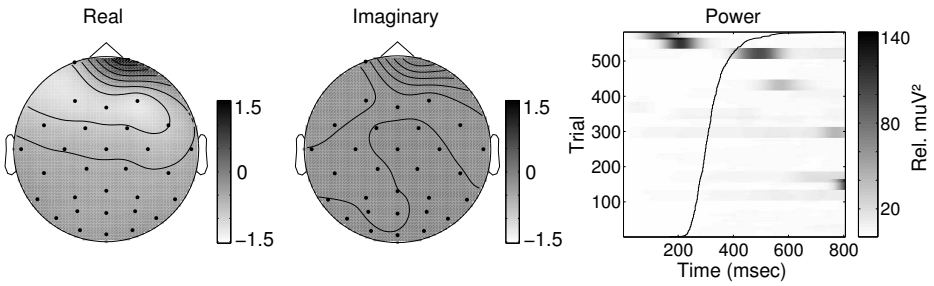

Fig. 5. Component 23 of the 5-Hz band was the most reliable in all three test conditions. The graphs display (from left to right) the real and imaginary parts of the component's complex scalp map, and its 5-Hz power ERP image, respectively (similar to Fig. 4). ERP image and scalp maps indicate that this component can be linked to a right eye artifact (possibly a right eyelid twitch) with a very sparse activity pattern. The small imaginary part of the complex scalp map indicates a low degree of spatio-temporal dynamics for this component.

compositions was always significantly higher than with its second-best matching component. This is illustrated in Fig. 2 for three example components obtained in the bootstrap data condition.

Reliable complex components were found under each of the three test conditions. However, the number of reliable components (out of 31 components in total) varied across conditions, with the bootstrap condition producing 16, the shuffling condition 28, and the initialization condition 11; see Fig. 3 for details. The reliable components constituted nested subsets: All components that were reliable in the weight initialization condition were also reliable in the bootstrap data condition, and all components reliable in the bootstrap data condition were also reliable in the training data order condition.

Among the reliable components, we found physiologically plausible components that were closely linked to behavior, e.g., the motor-response related component in Fig. 4, and 'artifactual' components like the right eye blink related component in Fig. 5. Some reliable components showed a clear phase shift across electrode positions with highest signal energy in the associated component scalp maps (Fig. 4), indicating an activity pattern with a strong spatio-temporal dynamics. Other reliable components did not exhibit such a phase shift (Fig. 5), showing that complex ICA may also produce near-static scalp maps, if appropriate for components of the data.

5 Discussion and conclusion

Complex ICA [1] applied to EEG recordings produces physiologically plausible and behaviorally relevant components. We have demonstrated here the degree of reliability of such components in the 5-Hz band. These results are complementary to the physiological and behavioral evidence that complex ICA may be used to faithfully model brain processes. Some of the reliable components showed phase shifts across electrode positions in the associated complex scalp maps that could not have been obtained using standard time-domain ICA methods. This finding suggests that complex ICA for EEG

signals can non-invasively measure the spatio-temporal flow patterns of cortical activation. It remains to be shown that these results extend also to other frequency bands.

We have shown that matching complex components across decompositions by means of their activity time course correlations is an effective way to investigate the effects of several variabilities on the results produced by the complex ICA algorithm. Variability in the data set, as implemented by resampling techniques, may be regarded as the variation of highest interest, since it tests reliability by generating data that might have been measured instead of the original data. It is reassuring that under this test about half of the 31 separated complex ICA components proved reliable. It remains an open question why we found a higher fraction of (one-dimensional) independent components than reported in [4]. This could, e.g., be due to the different algorithms or data sets used, or to our use of a 'global' instead of a 'local' approach. It appears unlikely that we have mistaken some multidimensional components for one-dimensional components, since the reliability threshold was chosen to be fairly high. Varying the training data order resulted in even smaller variations in the ICA results. Duann et al. [5] obtained even higher reliability, which might be attributed to differences in algorithm, data set, or training parameters. Varying the initial conditions of the algorithm resulted in a much larger variability in the outcome, which might not be surprising since global convergence has not been proven for ICA algorithms (including complex ICA). Nevertheless, it is remarkable that a significant number of components remained highly reliable even under this perturbation.

The methods investigated here provide complex ICA brain signal analysis with a quantitative indication of the numerical stability of components. Further studies are needed to confirm whether the quantitatively reliable components always coincide with components having meaningful physiological interpretations and covarying with subject behavior.

References

1. J. Anemüller, T. J. Sejnowski, and S. Makeig. Complex independent component analysis of frequency-domain electroencephalographic data. *Neural Networks*, 16:1311–1323, 2003.
2. A. Arieli, A. Sterkin, A. Grinvald, and A. Aertsen. Dynamics of ongoing activity: Explanation of the large variability in evoked cortical responses. *Science*, 273:1868–1871, 1996.
3. H. Berger. Über das Elektroencephalogramm des Menschen (On the electroencephalogram of man). *Archiv für Psychiatrie und Nervenkrankheiten*, 87:527–570, 1929.
4. F. Meinecke, A. Ziehe, M. Kawanabe, and K.-R. Müller. A resampling approach to estimate the stability of one-dimensional or multidimensional independent components. *IEEE Transactions on Biomedical Signal Processing*, 49(12):1514–1525, December 2002.
5. J.-R. Duann, T.-P. Jung, S. Makeig, and T. J. Sejnowski. Consistency of infomax ICA decomposition of functional brain imaging data. In *Proceedings of the fourth international workshop on independent component analysis and blind signal separation*, pages 289–294, Nara, Japan, April 2003.
6. A. J. Bell and T. J. Sejnowski. An information maximization approach to blind separation and blind deconvolution. *Neural Computation*, 7:1129–1159, 1995.
7. S. Makeig, M. Westerfield, T.-P. Jung, S. Enghoff, J. Townsend, E. Courchesne, and T. J. Sejnowski. Dynamic brain sources of visual evoked responses. *Science*, 295:690–694, 2002.